Gerda

Progress Report to the LNGS Scientific Committee

Version 1.1

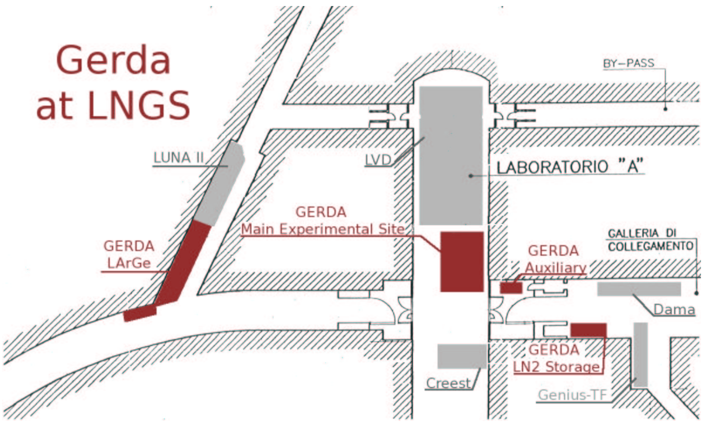

March 2005

I. Abt [j], M. Altmann [j], A.M. Bakalyarov [i], I. Barabanov [g], C. Bauer [c], M. Bauer [l], E. Bellotti [f], S. Belogurov [g,h], S.T. Belyaev [i], A. Bettini [k], L. Bezrukov [g], V. Brudanin [b], V.P. Bolotsky [h], A. Caldwell [j], C. Cattadori [a,f], M.V. Chirchenko [i], O. Chkvorets [c], E. Demidova [h], A. Di Vacri [a], J. Eberth [d], V. Egorov [b], E. Farnea [k], A. Gangapshev [g], P. Grabmayr [l], G.Y. Grigoriev [i], V. Gurentsov [g], K. Gusev [b], W. Hampel [c], G. Heusser [c], W. Hofmann [c], L.V. Inzhechik [i], J. Jochum [l], M. Junker [a], S. Katulina [b], J. Kiko [c], I.V. Kirpichnikov [h], A. Klimenko [b,g], K.T. Knöpfle [c], O. Kochetov [b], V.N. Kornoukhov [g,h], R. Kotthaus [j], K. Kröninger [j], V. Kusminov [g], M. Laubenstein [a], V.I. Lebedev [i], X. Liu [j], H.-G. Moser [j], I. Nemchenok [b], L. Pandola [a], P. Peiffer [c], R.H. Richter [j], K. Rottler [l], C. Rossi Alvarez [k], V. Sandukovsky [b], S. Schönert [c], S. Scholl [l], J. Schreiner [c], U. Schwan [c], B. Schwingenheuer [c], H. Simgen [c], A. Smolnikov [b,g], F. Stelzer [j], A.V. Tikhomirov [i], C. Tomei [a], C.A. Ur [k], A.A. Vasenko [h], S. Vasiliev [b,g], D. Weißhaar [d], M. Wojcik [e], E. Yanovich [g], J. Yurkowski [b], S.V. Zhukov [i], G. Zuzel [c]

[a] INFN Laboratori Nazionali del Gran Sasso, Assergi, Italy
[b] Joint Institute for Nuclear Research, Dubna, Russia
[c] Max-Planck-Institut für Kernphysik, Heidelberg, Germany
[d] Institut für Kernphysik, Universität Köln, Germany
[e] Jagiellonian University, Cracow, Poland
[f] Università di Milano Bicocca e INFN Milano, Milano, Italy
[g] Institute for Nuclear Research of the Russian Academy of Sciences, Moscow, Russia
[h] Institute for Theoretical and Experimental Physics, Moscow, Russia
[i] Russian Research Center Kurchatov Institute, Moscow, Russia
[j] Max-Planck-Institut für Physik, München, Germany
[k] Dipartimento di Fisica dell'Università di Padova e INFN Padova, Padova, Italy
[l] Physikalisches Institut, Universität Tübingen, Germany

Spokesperson: S. Schönert,
(Stefan.Schoenert@mpi-hd.mpg.de)
Co-Spokesperson: C. Cattadori
(Carla.Cattadori@lngs.infn.it)
Technical Coordinator: K.-T. Knoepfle
(ktkno@mpi-hd.mpg.de)

Contents

1 Executive summary

This document summarizes the progress of the GERDA experiment which has been accomplished since October 2004. Most relevant issues and recent achievements are highlighted below:

- **Approval by LNGS:** During the last general GERDA meeting February 3-5, the director of the LNGS, Prof. Coccia, told the collaboration board that the experiment has been approved by the LNGS.

- **Underground locations for GERDA:** After various iterations with the LNGS scientific and technical management, and in close contact with members of the CUORE and LVD collaborations, the locations of GERDA could be decided. The main experimental facility will be located in Hall A of the LNGS in front of the LVD detector. A second location, the LARGE–Facility, will be sited in the interferometer tunnel, adjacent to LUNA-II.

- **Technical Proposal:** A first version of a technical proposal is available. Its purpose is to facilitate the engineering integration and to provide a coherent plan of all GERDA facilities. This document serves as well for risk assessments and safety reviews.

- **Funding situation:** Funding requests to the INFN Commissione–II and to the BMBF Verbundforschung Astro–Teilchenphysik have been submitted in 2004 and 2005 respectively. In February, Commissione–II of INFN approved GERDA and assured the provision of funds for the water tank construction in 2005. A preliminary decision of the BMBF is expected in April.

- **Collaboration forming:** A new group (M. Hult) at the Institute for Reference Materials and Measurements (IRMM) in Geel (Belgium) joined the GERDA Collaboration. This group operates three low-level Germanium gamma ray spectrometers in the underground laboratory HADES, located in Mol (Belgium), thus substantially enlarging the capabilities of GERDA for material screening. Given the vicinity of HADES to the crystal growing and diode producing companies, this group will provide essential logistic support for the production and underground storage of enriched diodes. Contacts with other groups are pursued with the goal to further strengthen the expertise and financial resources of the collaboration. The close cooperation with the MAJORANA collaboration is continuing and formalized with a LoI.

- **Schedule:** The time schedule as presented in the GERDA proposal targets the start of data taking during summer 2006. Some of the sub-projects have accumulated delays with respect to the original schedule, however, most of them do not have an impact on the scheduled start of data taking. On the 'critical path', however, are the cryogenic vessel and the installation of the water Cerenkov detector. Potential delays in the availability of funding for the water Cherenkov detector would require to shift in time the mounting of this part of the detector after completion of Phase I.

This would interfere with physics data taking of Phase II. An updated schedule will be worked out during the next months once all necessary information is available.

The GERDA collaboration is fully operational and major technical progress has been achieved. The GERDA project is broken down in (currently) 11 different tasks and each task is implemented by a task group as listed in the table below. This report emphasizes the work which has been done during the last six months to get timely the experimental infrastructure in place. Significant progress has also been achieved in other areas and will be reported in later documents.

Table 1: Task groups and respective leaders

TG-1: Modification and test of existing Ge diodes	S. Schoenert
TG-2: Design and production of new Ge diodes	A. Caldwell
TG-3: Diode readout and signal processing	C. Cattadori
TG-4: Cryogenic vessel	K.T. Knoepfle
TG-5: Infrastructure on top of vessel	I. Abt
TG-6: Water vessel and muon veto water Cherenkov	A. Bettini
TG-7: Scintillator muon veto on top of vessel	V. Egorov / A. Smolnikov
TG-8: Infrastructure & logistics for Gerda	M. Junker
TG-9: DAQ Electronics & software	B. Schwingenheuer
TG-10: Simulation and background studies	L. Pandola
TG-11: Material screening	W. Hampel

2 Locations of Gerda

The main experimental site of the Gerda experiment is located in Hall A in front of Lvd. In addition, the Gerda LArGe facility for detector manipulation, handling and testing for Phase I, is located in the interferometer tunnel adjacent to Luna II (former Lens). The LN_2 storage area and an auxiliary system area are both located in the TIR tunnel section between Hall A and Hall B. All Gerda locations in the underground laboratory are indicated in Fig. 1. Additional space is required in the above ground laboratory.

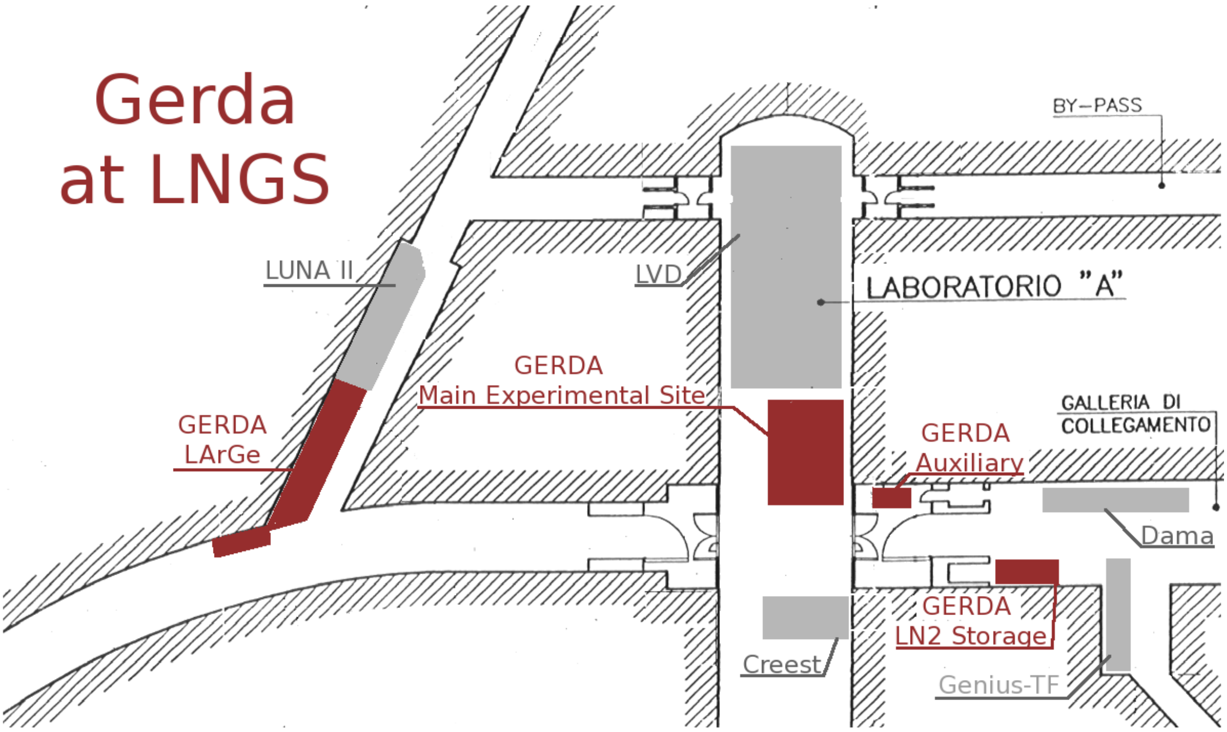

Figure 1: Location of the GERDA experiment in Hall A.

2.1 The main experimental site of Gerda

The layout of the main experimental site is shown in Fig. 2 and 3. The water vessel containing the cryostat with the germanium detectors is placed close to the TIR tunnel as far as possible from the Lvd experiment. A three floor laboratory building called super-structure is placed between Lvd and the Gerda water vessel.

The ground floor of the super-structure contains the machine room with vacuum and cryogenic equipment as well as the equipment for the water treatment. The first level hosts the service area which consists of the control room, a laboratory for on site repair and maintenance and a DAQ-position for the Lvd experiment. The Phase II detector laboratory dedicated to the handling of the detectors for Phase II is place on the second

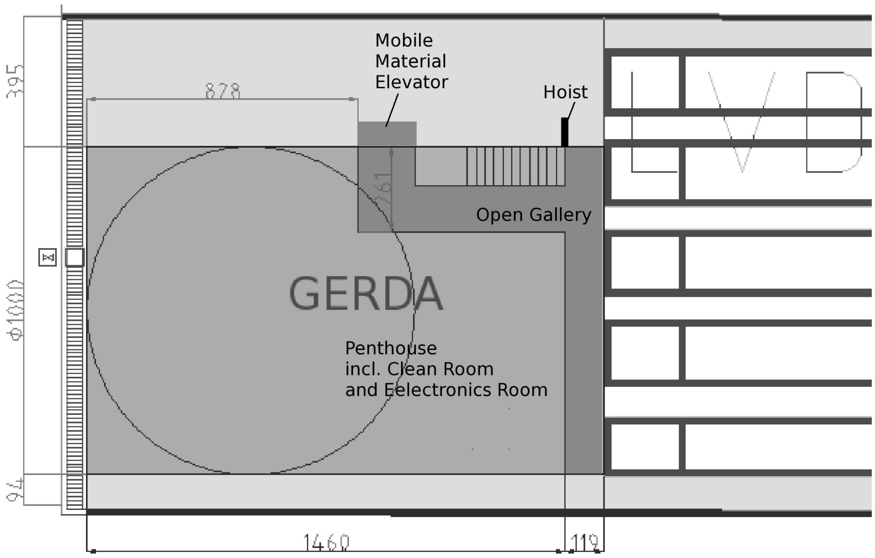

Figure 2: Layout of the Main Experimental Site of GERDA in Hall A. All Dimensions are in cm.

floor. The third level named penthouse in the following extends over the whole water vessel and hosts a clean room for detector string assembly and an electronic area for front end electronics. A stair case incorporated in the super-structure gives access to open galleries on all levels placed between GERDA and LVD. These galleries of a width of 1,20 m allow the access to the experimental areas of GERDA and serve also as emergency exits from the LVD experiment.

The super-structure is mechanically decoupled from the water vessel and the cryostat. The admitted load for all floors is 1000 kg/m^2 while in the area of the inner lock a load of 6000 kg in total is foreseen. In this area the support structure of the penthouse keeps a clearance of ϕ=150 cm for the neck of the cryostat.

An electrical hoist with a maximum load of 1500 kg is mounted on the third level. In addition all levels have a docking position which allows to bring in bulky equipment like furniture with a mobile elevator (see Fig. 3). An additional material lift (max. 200 kg) will connect the clean room areas of the Penthouse and the Phase II Detector Laboratory.

As can be seen from Fig. 5 the vertical height of GERDA allows for the passage of the crane from the north to the south of Hall A. However the hook of the crane must be moved to a lateral position. Safety systems will be installed and operational procedures will be implemented in order to avoid collisions between the hook and the GERDA experiment.

Sensors for fire, temperature and oxygen loss must be provided in all rooms. These sensors will be inserted in the LNGS supervision system.

An exhaust line for blow off of nitrogen gas generated during the normal operation

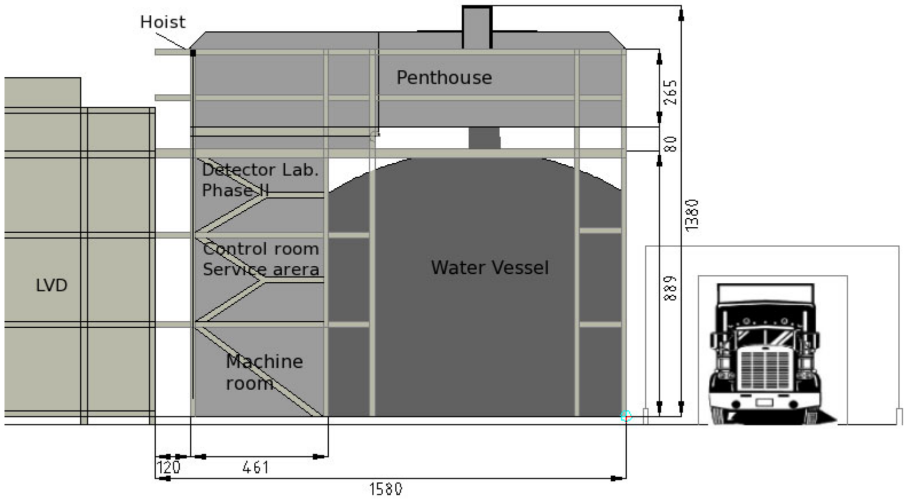

Figure 3: Lateral view of the GERDA experiment in Hall A. All dimensions are in cm.

brings the nitrogen to the exit of the underground laboratory. This duct also takes the exhaust of the fume hoods in the penthouse and in the Phase II Detector Laboratory.

2.2 Liquid nitrogen storage and auxiliary equipment

The LN_2 storage area is indicated in Fig. 1. Two 4 m^3 dewars entirely made out of stainless steel are mounted here. Super-insulated lines connect these dewars to the main experimental site. The consumption of LN_2 is estimated to be of about 4 m^3 per week. The main electrical switchboard of the experiment and part of the cryogenic equipment, which cannot be placed in the machine room of the Super-Structure is located outside Hall A as in Fig 1.

2.3 Space in the 'above ground' laboratory

The experiment is controlled from the 'above ground' laboratory from a dedicated external control room. From this location the complete status of the experiment can be monitored continously. Experimental activities like testing PMTs and electronics are carried out in a dedicated external experimental area.

3 Experimental infrastructures

3.1 The cryostat

The cryostat contains the liquid nitrogen (LN) or argon (LAr) in which the Ge diodes are operated. The cryogenic liquid serves simultaneously as a shield against the remnants of the external γ background penetrating the surrounding water shield and the cryostat's own radioactivity. The baseline is a super-insulated cryostat manufactured predominantly from low-radioactivity copper; the fall-back solution is a super-insulated stainless steel cryostat with an internal lead or copper shield in the cold volume.

Recent efforts have focused on finalizing the specifications for the copper cryostat as well as to measuring the radio purity of materials to be used for the cryostat.

There are now two design studies for a copper cryostat available which differ in the way the inner vessel is attached to the outer shell; it might be either hanging at the neck of the cryostat or resting on fiber glass reinforced plastic pads. While the former solution is more elegant the latter has the advantage that the copper-stainless steel weld is less loaded; it also fulfills all requirements on earthquake tolerance (0.6 g) and evaporation rate (<0.2%/day). The final decision will depend on the outcome of welding tests.

The required radiopurity of the copper has been verified so far for the copper grade NOSV only which had been delivered by the Norddeutsche Affinerie AG to the MPI Heidelberg. The required DHP copper grade is a phosphorus-deoxidized product; it can be produced from the NOSV grade by being alloyed with 0.015 to 0.040 (mass)% of phosphorus. Technically, a phosphorus-copper granulate with 10 (mass)% of P is added in the electrically heated melting furnace to the NOSV material. Thus the radiopurity of the resulting DHP copper can be deduced most easily from the radiopurity of the phosphorus-copper granulate. A preliminary upper limit of its ^{228}Th activity is 10 mBq/kg; hence assuming an addition of 3 g P-Cu granulate to 1 kg of NOSV grade copper will increase its radioactivity by less than 30 μBq/kg which is less than 1.3 times the specified value. Work is in progress to improve the sensitivity of the measurements and if necessary to reduce the ^{228}Th content of the granulate.

The radiopurity of one type of thermal insulation, NAC-2 cryo-laminated superinsulation foil with bonded space material according to HERA/DESY specifications, has been measured to be less than 50 mBq/kg (upper limit). Assuming 20 layers of a density of 24.2 g/m^2, this would increase the radioactivity budget by less than 140 μBq/kg. Thus, a more sensitive measurement is needed.

Ongoing activities to prepare the production of the copper cryostat include

- final production drawings for both types (hanging/resting) of copper cryostat
- electron beam welding tests of DHP copper
- electron beam welding tests of DHP copper and stainless steel (ss)
- TÜV certification for Cu-Cu and Cu-ss welding
- production of part of a hemisphere from Cu segments including a Cu-ss joint
- establishment of procedure for pressure vessel certification.

In parallel, screening of materials to be used for polishing the copper cryostat is continued, and various options for the cleaning and passivation of copper surfaces have been investigated.

On January 31, the process of purchase of the copper cryostat has commenced by publishing in the *'Supplememnt of the Official Journal of the European Union'* a *'Prior Information Notice'* - SIMAP-MPI-K 31 Jan'05 ID:2005-002331 - which invited parties to express their interest to tender for the copper cryostat and infrastructure. By March 15, the deadline for receipt of participation requests, expressions of interest from more than 7 companies including Linde and Air Liquide have been received. The award procedure will start immediately by sending the technical specifications to the interested companies and asking for their respective quotes. It appears that almost all companies will tender for either the mechanical work or the cryogenic lot since no single supplier has the needed expertise in both fields.

The safety review has been started already last year by handing out a preliminary fabrication drawing to our Italian colleagues. Final drawings will be available after Easter, and the Technical Proposal discusses also some safety aspects that are specific for the cryostat-water vessel system. If the safety review and the order of the cryostat will be done by May and the welding tests are successful, the cryostat could be delivered in January 2006.

3.2 The water tank

The water tank (WT) will host the super-insulated cryostat, provide shielding against external radiation and serve as a water Chrenkov detector to suppress cosmic ray muons. It will be 8.9 m in height and 10 m in diameter. Its main features are described in Tab. 2 and its structure diplayed in Fig. 4

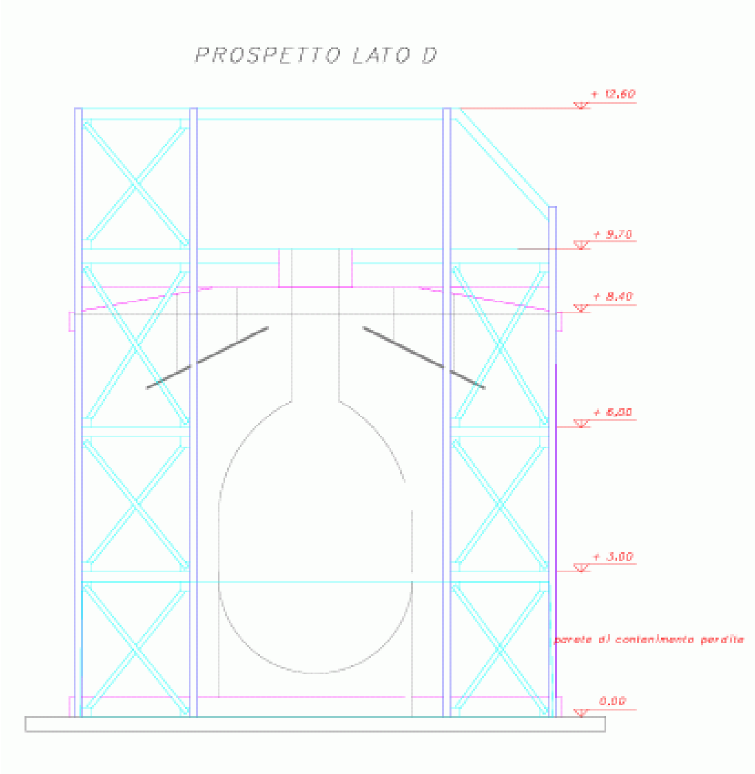

Figure 4: View from the TIR tunnel onto super-structure and water tank.

Its purpose is to contain the ultra pure (18 MΩ/cm) water produced by the Borexino plant that will be carried at the GERDA site through an appropriate pipe. The WT will be projected following the API 650 regulation, and the Eurocodice 8 for the seismic acceleration, and built following the Italian safety regulations and LNGS Laboratory rules. The WT construction is planned to start in autumn 2005, from a qualified company that will win the tender procedure. The Borexino WT tank is a reference concerning the safety aspects and the quality of the final product. A structure holding $\approx$ 80 – 100 PMTs (8” diameter) to read out the Cerenkov light produced by the muons crossing the water, will be fixed at the WT shell inner side. Due to its dimensions the WT will be built on site.

The GERDA water tank provides the outer shielding shell for the GERDA experiment which has the generic thickness of 3 m. The vessel houses in its center the cryostat in which the Ge diodes are operated. The water serves in addition as Cherenkov medium for the muon veto system.

Table 2: GERDA Water Tank main features

Reference regulation for structural project:	API650
Further verification for seismic hazards:	Eurocodice 8
Quality certification of construction process:	ISO9001
Quality certification required for company:	ISO14001
Tank height / external diameter:	8.9 m / Ø 10.0 m
Height of the water level:	8.4 m
Effective capacity (m^3):	633 m^3
Water tank bottom:	flat, plates head welded
Water tank roof:	conical from the shell, (Ø 4.5 m)
Water tank shell:	cylindrical, plates head welded
Water tank sheet-metal plates:	$\approx$2 m
Angle between shell and roof:	$\approx 6^\circ$
Bottom reinforcement:	yes, at 1 feet level
Reinforcement rings along the shell:	yes, 1 or 2
Water tank Material:	Stainless Steel AISI 304 L or 304 LN, or Carbon Steel plus appropriate coating
Thickness of the shell:	12 to 9 mm
Connections between plates:	Welded
Welding type:	External MIG, internal TIG without filler metal
Welding certification:	certified by the executing company, fully X-ray tested
Approximative length of welds:	400 m
Flanges	
1 DN 5000	with DAVIT lateral at bottom
1 DN 1800	in roof for cryostat neck
6 DN 500	in roof for monitoring control of level, pressure, temperature incl. spares
1 DN 300	for total drain compensation
2 DN 250	in roof for photomultiplier cables
1 DN 200	to drain tank completely in 20 h
2 DN 32	lateral for water recirculation
Weight of water tank (tons):	(<20 tons)
Weight of filled water tank:	(600 tons)
Operational over/underpressure:	$\pm$20-30 mbar
Safety device:	pressure/depressure $\pm$20-30 mbar
Water recirculation:	yes, 2-3 m^3/h
Water recirculation plant:	deionization, Radon stripping, particulate removal

3.3 The infrastructure on top of tank

The overall dimensions of the experiment were adjusted to optimally use the clearance of hall A. The current design as depicted in fig. 5 allows for sufficient clearance above the lock to facilitate the vertical lift necessary for the detector insertion procedure without significantly reducing the depth of the water shield.

The overall infrastructure of GERDA was modified to include a backside house. The penthouse design was adjusted accordingly preserving the previously defined functionality. Technical specification were firmed up and are included in the technical proposal.

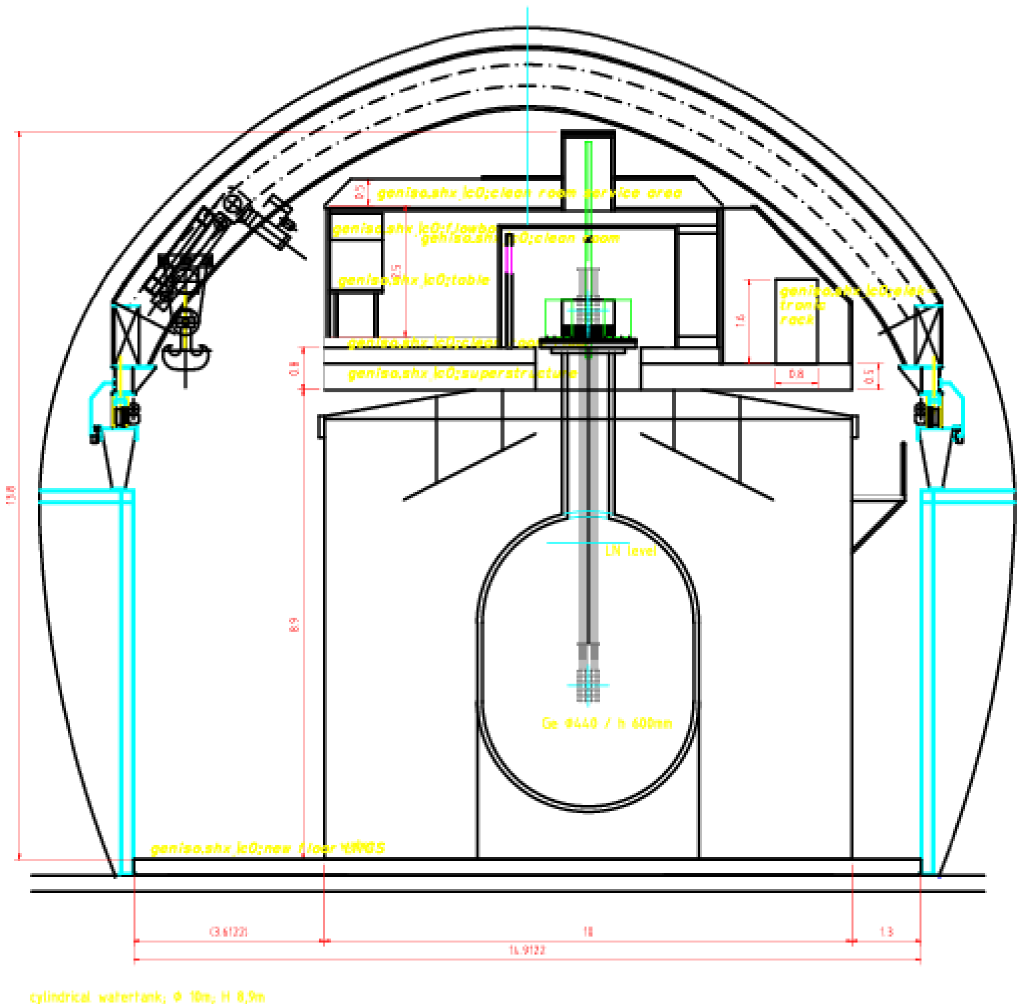

Figure 5: Vertical cut through the center of the experiment looking from the TIR tunnel.

4 Modification and testing of enriched detectors

The following work packages have been defined and are currently carried out by task group 1 (TG1) in order to prepare and test the enriched germanium diodes timely for their use in Phase-I of GERDA:

WP1: New underground infrastructures (LARGE–FACILITY): refurbishment of the LENS LOW-BACKGROUND FACILITY for its use as an underground detector laboratory and for investigation of background suppression by detection of liquid argon scintillation light.

WP2: Characterization of the existing enriched germanium diodes in their original HDM and IGEX cryostat configuration with calibration sources.

WP3: Design & construction of low-mass detector support and electrical contacts; mounting of the diodes in new support system for operation in liquid nitrogen/argon.

WP4: Mounting and contacting diodes in new support structure; characterization of detector performance with respect to signal response and radioactive background.

The activities of WP1-3 are pursued in parallel. However, priority is currently given to the modification and refurbishment of the underground barrack and its infrastructures for handling detectors in a clean-room environment (WP1). WP2 is being carried out continuously until all detectors are removed from their cryostat and mounted into their new support structure. WP4 is not addressed in this report, as it will start only after completion of WP1 and WP3.

4.1 The underground detector laboratory (LARGE)

The former LENS LOW-BACKGROUND FACILITY (LLBF) is currently converted to an underground detector laboratory, named the LARGE–FACILITY. Figure 6 displays the floor plan of the new laboratory and its infrastructure. The purpose of the facility is to provide underground space to modify and test the existing enriched detectors previously used in the Heidelberg-Moscow (HDM) and IGEX experiments. It further serves to study the novel background suppression technique by measuring simultaneously the scintillation light of liquid argon in which the diodes are submerged. The new setup employs the low-activity copper, steel and polyethylene of the LENS shielding system. Dismounting of the system was carried out during November 2004. About 80 tons of shielding material were removed from underground and transported to a company for machining according to the new design. After completion of machining, the copper was immediately carried back underground in December to minimize cosmogenic exposure with and overall time of exposure above ground of less than four weeks. The machined steel and polyethylene as well as the new low-activity lead is ready for transportation and will be shipped underground, in early April after completion of the barrack refurbishment. Figure 7 shows the 3D construction drawing of the LARGE setup.

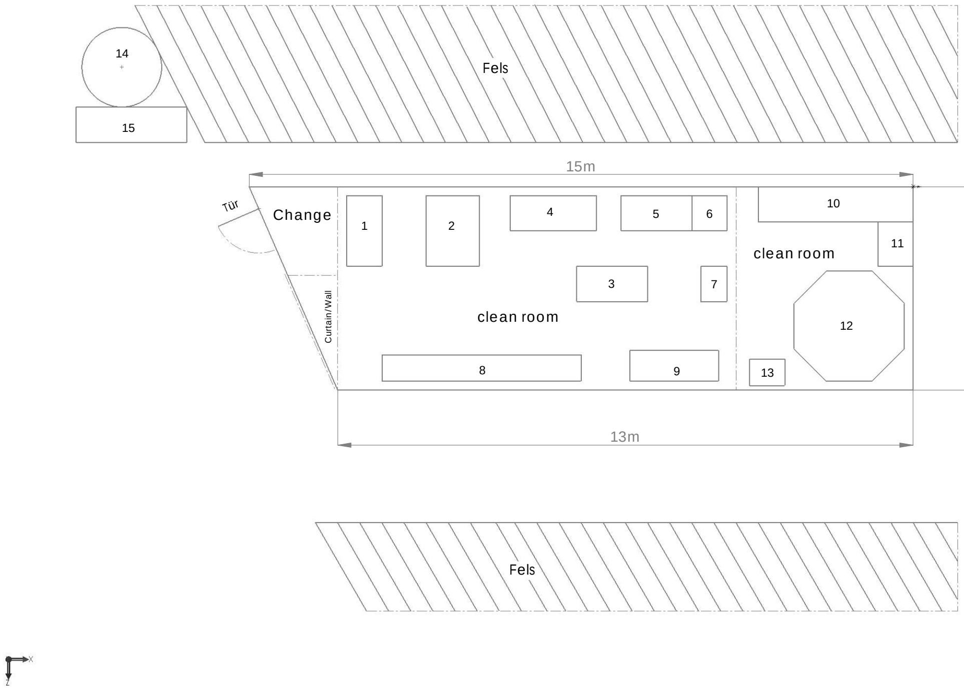

Figure 6: Floor plan of the LArGe–Facility: 1) fume hood, 2) washstand and DI water preparation, 3) mounting table (movable), 4) clean bench, 5) Rn-free clean bench (nitrogen atmosphere), 6) nitrogen dewar (integrated into 5) for diode tests, 7) DAQ for 6, 8) storage shelfs, 9) desk, 10) liquid/gaseous argon handling system, 11) access ladder to top of 12, 12) LArGe shielding system, 13) DAQ, 14) liquid argon storage, 15) liquid argon purification system.

Modification of the Lens barrack commenced in February and will be completed at the end of March. New laboratory equipment (fume hood, clean bench, radon-free clean bench, and further general infrastructures) has been ordered or is under construction, and will be installed during April and May. Detector modification inside the clean room area of the LArGe–Facility will start in May. After completion of the radon lock and cryogenic vessel, the LArGe prototype system (Fig. 7) is targeted for completion in autumn 2005.

4.2 Characterization of enriched detectors

The goal of this activity is to obtain detailed information about the existing detectors concerning their performance prior to their modification such as energy resolution, absolute efficiencies, dead layer and pulse shape information. The detectors from the former Heidelberg-Moscow experiment (HdM) have been carefully investigated over the last months. For example, the measured energy resolutions at 2.614 MeV are 3.9 (3.0) keV (Detector-1 (D1)), 2.7 (3.4) keV (D2), 3.0 (3.0) keV (D3), 2.8 (3.5) keV (D4) and 3.1

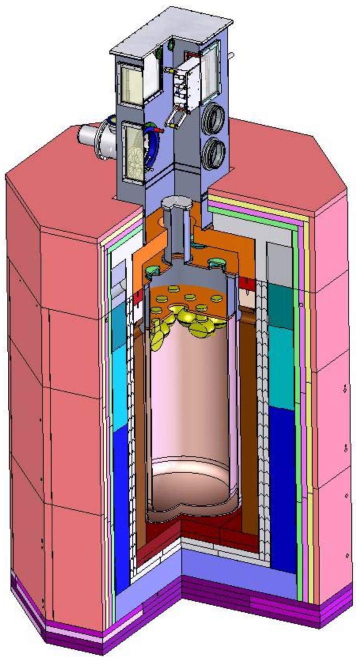

Figure 7: 3D drawing of the LArGe prototype system. (Compare item 12 in Figure 6). The re-machined Lens shield will used in this setup and is now ready for assembly.

(3.4) keV (D5). In brackets are given the resolution as observed during their operation in the HdM experiment. Apart from D1 which had been received 'warm' from the former user, all detectors exhibit an energy resolution which is as good or even better than in the past. Ongoing measurements are scans with a ^{133}Ba source for determining the dead layer and with a ^{60}Co for absolute efficiency determination. First pulse shapes have been sampled for testing candidate flash-ADCs.

4.3 Design & construction of low-mass detector support

Based on the results of our screening measurements, only few materials achieve the required purity levels and are considered as suitable materials for detector support and electrical contacts. Copper from our batch used in Lens [1] (impurity levels: ^{226}Ra (U) < 16 μBq/kg, ^{228}Th (Th) < 19 μBq/kg and ^{60}Co < 10 μBq/kg) is under consideration to be used for the detector support cage, single crystal silicon (^{238}U $< 3 \times 10^{-4}$ μBq/kg, ^{232}Th (Th) $< 1.2 \cdot 10^{-3}$ μBq/kg) for the inner core contact (Ortec type of contact), as well

[1] A new analysis of the copper measurements gave lower limits with respect to the numbers quoted in the Gerda report.

as elastic spring material. Furthermore, silicon is considered as an alternative material for the construction of detector support material. Teflon (^{226}Ra (U) $<$ 160 μBq/kg, ^{228}Th (Th)$<$ 160 μBq/kg) appears most suited as insulation material. Other materials, as for example micro-springs made out of Cu/Be in a copper housing for electrical contacts (total mass 0.1 g), alternative insulation materials (PEEK, Torlon), as well as rope materials (Tensylon) are being investigated for their impurity levels. Material and design studies as well as prototype machining of copper and silicon are ongoing.

5 New detectors for Phase II

For phase-II of GERDA the production of an additional ≈ 20 kg of ^{76}Ge-enriched detectors is planned, in order to further increase the sensitivity of the experiment by about a factor of three. Task group 2 is currently progressing on the following work packages:

- Procurement of $\approx 30 - 35$ kg of germanium, enriched to 86% in ^{76}Ge.
- Optimization of the enrichment technology with respect to increasing the product cleanliness and minimizing time above ground.
- R&D on increasing the yield of chemical purification step.
- Optimization of crystal production with respect to maximizing yield and minimizing activation by cosmic rays.
- Crystal production from the enriched material.
- Material tests at various steps of the production chain.
- R&D on detector technology (naked, segmented detectors).
- Fabrication of low-background Ge-detectors (segmented).

Germanium procurement is done in two steps: procurement of 15 kg of natural Ge ('test run'), and subsequently procurement of 30-35 kg of ^{76}Ge ('real run'). Both samples are produced in Siberia / Russian Federation. The 15 kg batch of natural (i.e. non-enriched) germanium, chemically purified to 99.9999%, is shipped in exactly the same way as the enriched sample. A specially designed protective steel container (PSC) which reduces activation by cosmic rays by about a factor of 20 is used for transportation. The 'test run' serves on the one hand to discover possible unforeseen problems and time-delays which might occur during transportation, customs, bureaucracy, handling, etc., which then could be avoided for the precious enriched sample. On the other hand, it is also used to tune the techniques and instruments employed for material quality checks and as a test batch for crystal production and detector fabrication. Procurement of the natural germanium has been successfully concluded; the natural sample was received at MPI Munich on March 7,

Figure 8: Unstacking the protective container which was used to shield the germanium from activation by cosmic rays during transport.

2005. Fig. 8 shows the dismantling of the PSC which after unloading of the germanium was sent back in order to be re-used for the transport of the enriched sample.

Production of the 30-35 kg sample of enriched ^{76}Ge was started in Siberia in February. The estimated production time is 6 months, i.e., the material should be ready for shipment in August/September. Due to R&D invested in co-operation with the manufacturer into tuning the employed equipment, it has been possible to increase the purity of the enriched material to $\approx 99.99\,\%$, substantially better than the $99.8\,\%$ which were originally quoted.

R&D on chemical purification has led to the promise of an improved technique which has a yield of more than 85%, to be compared to the $\approx 70\,\%$ of the standard procedure.

Discussions with the crystal grower are ongoing, with the aim of adapting their equipment and procedure towards achieving a high yield for our sample (which is extremely small compared to their usual batch sizes).

Monte Carlo simulations with the MaGe Geant4 framework are ongoing to study the performance and segmentation schemes of detectors both in close array packings as well as in combination with simultaneous suppression by liquid argon scintillation readout.

Background reduction of one order of magnitude and more appears feasible by exploiting the information on the charge deposition topology.

Segmented prototype detectors for operation in liquid nitrogen have been ordered and are currently being produced. They are not yet low-background and will be used for test measurements, in order to optimize the segmentation scheme and to develop readout and analysis tools.

6 Electronics

6.1 Analog electronics

The activity of TG-3 ('Diode read out and signal processing') is currently focused on the selection of the analog front-end electronics. For Phase I, two front-end solutions are pursued and under test:

(1) Cold JFET and feed-back components connected to a warm integrated preamplifier through 5 m cable: this solution has been successfully tested and it works when compensating for the capacity of the long cables, at the expenses of the bandwidth of the full read-out chain. The measurements of the equivalent noise charge (ENC) in this configuration when the JFET is sinked in LN are ongoing and will soon be available. Also the noise pick up and cross talk between different channels have to be further investigated. Two couples of JFET + amplifier could be used, either the Philips BF862 JFET associated to the custom developed MARS/AGATA preamplifier or the IF1331 JFET associated with the EURISYS PSC823C preamplifier. All these devices have been selected or developed in the framework of the AGATA project. The output of the amplifier could be either single ended or differential. From preliminary but encouraging measurements performed on Philips BF862 coupled to the MARS/AGATA integrated preamplifier through 3.5 m of RG62 coaxial cable, a rise time of 60 ns and an ENC of 165 electrons RMS has been obtained with the JFET at room temperature and a 23 pF detector at the input. With the JFET at lower temperature the ENC is expected to decrease.

(2) A JFET-based monolithic preamplifier fully integrated on silicon together with the front end JFET. This preamplifier have been developed for liquid argon calorimetry purposes and then, given the outstanding noise performances, modified for spectrometry applications. They are produced using a buried-layer technique in which p^+ islands (buried layers) are diffused into an n-type substrate. The IPA4 preamplifiers are under test at LN temperature.Their reference noise figure is 250-300 electrons RMS for an input capacitance of 35 pF at 3 μs shaping time. This device is very promising for GERDA application as the signal will be transmitted along the 5 m cable from the crystal to the digitizer, already amplified. It works at LN temperature and ENC in LN are ongoing, as well as the study of its mounting in this specific application to minimize the cross talk between different channels.

6.2 Digital electronics

The first goal of TG-9 is to decide on the FADC which will be used by GERDA. The choice will affect the DAQ structure considerably. The general requirements are an *effective* number of bits of at least 10 and a sampling rate of typically 100 MHz. In addition, a system for $\mathcal{O}(100)$ channels should be easy to configure with respect to the synchronization of all channels and the generation of a common trigger.

Four solutions are currently considered: the Struck SIS3301 (8 channel VME card), the Joerger VTR10014 (8 channel VME card), the XIA DGF Pixie-4 (4 channel PXI card) and the INFN Padova MD^{2}S readout system (NIM card for ADC and PCI card for digital signal processing). Tests foreseen in the next months concentrate on the analoge performance of the cards. These include an estimate of the effective number of bits, temperature stability and long term stability. The final decision for the readout system is expected for summer 2005.

7 MC simulations and background studies

The main tasks of the TG-10 ("Simulations and background studies") are to: (1) simulate energy depositions in Ge crystals both from $0(2)\nu2\beta$ decays and from background sources, in order to develop optimized 'cut strategies' for background reduction and signal acceptance, (2) simulate the energy deposition in other parts of the GERDA set-up and study the background suppression by measuring scintillation light in case of liquid argon, (3) simulate test stands from different institutes and compare the outcome with real data, so as to validate the simulation of physics processes, (4) optimize the GERDA geometry, including shielding, detector orientation, crystal segmentation, on the basis of the background and signal simulations, (5) simulate pulse shape and mirror charges etc., and develop filters to further reject background.

7.1 The MaGe package

MaGe is a Monte-Carlo simulation package for the search of $0\nu2\beta$ decay in ^{76}Ge, initiated by the Majorana collaboration, now developed by a joint group of Majorana and GERDA collaborators. A common framework has the great advantage of merging the efforts of experts from both groups, and allowing the simulation results to be validated with data coming from independent experiments. MaGe is based on Geant4, a software well-established and widely used in the physics community. This, combined with the object-oriented coding technique, makes the MaGe toolkit solid on the long-term, and very flexible: the tasks can be easily broken down into many sub-groups and developers, and several different geometries and databases can be supported, ensuring a certain independence of the two groups, which is critical to perform a sensible cross-check of the results. A complete GERDA specific geometry, including shielding, crystal array and supporting structures, has been implemented in the MaGe package. Dimensions and other parameters can be configured and tuned at run-time, without recompiling the whole package, making it accessible to new users.

7.2 Muon background studies

The cosmic ray background for the Phase I (9 crystals) was simulated with MaGe in order to quantify the background index at $Q_{\beta\beta}$ and to optimize the veto system (plastic scintillator above the set-up and instrumentation of the water tank as a Čerenkov detector). The assumptions, the details of the simulation and the results are discussed in an attached Gerda internal note (GSTR-05-003).

The background index at $Q_{\beta\beta}$ in the case of no cuts is $3.3 \cdot 10^{-3}$ cts/keV/kg/y; this is reduced to $1.0 \cdot 10^{-3}$ cts/keV/kg/y if crystals are used in anti-coincidence. The μ background index can be further lowered by making use of the dedicated muon vetos: if only the crystal anti-coincidence and the top μ-veto are used, the achievable background index ranges between $(5-9) \cdot 10^{-4}$ cts/keV/kg/y. The plastic scintillator should be placed immediately above the water tank: in this way the background index for a $5{\times}5$ m^2 plate (+ crystal anti-coincidence) can be as low as $4.4 \cdot 10^{-4}$ cts/keV/kg/y, which would suffice the requirements for Phase I. With the water tank instrumented as a Čerenkov detector, using a very standard design and a modest photo-cathode coverage (0.5%, 80-100 PMTs), muons are effectively vetoed and the background is reduced well below 10^{-4} cts/keV/kg/y ($< 3 \cdot 10^{-5}$ cts/keV/kg/y at 95% CL), meeting also the requirements for Phase II.

From the above numbers we conclude that the water μ-veto is not strictly necessary for Phase I, however, we are convinced that it should be installed already for Phase I. This is because (1) the plastic scintillator and water Cerenkov detector will provide redundancy between the two systems (and a wider "safety margin"), and even more important, (2) the mounting of the PMTs in between Phase I and II which would lead to a serious interference with physics data taking. The water μ-veto is definitely needed for Phase II; also in this case the simultaneous presence of the top μ-veto is very welcome because of redundancy and complementarity.

7.3 Background studies from radioctive decays

Background events from different radioactive sources, including ^{60}Co, ^{208}Tl, ^{210}Pb and ^{214}Bi are generated in the crystals or the supporting structures. Recent studies focused on the γ background suppression of sources close to the detectors (eg. holder, surface, contacts) and bulk contaminations by using anti-coincidences between crystal segments in a closed packed geometry of 21 crystals of 2 kg each. For a $6_\phi \times 3_z$ segmented crystals, as considered for Phase II, the fraction of radioactive decays that deposit an energy in one segment only within a 10 keV window around $Q_{\beta\beta}$, varies between 10^{-4} to 10^{-5}. The results are given in Tab. 7.3.

The configuration of the crystals (size, segmentation, position and their actual number) is under study in order to optimize the setup for background reduction using the anti-coincidence.

Source	Location	Fraction in [$Q_{\beta\beta} \pm 5$ keV]
^{60}Co	Holder	$0.7 - 2.4 \times 10^{-5}$
^{208}Tl	Holder	1.5×10^{-4}
^{214}Bi	Holder	2.7×10^{-5}
^{68}Ge	Crystal	2.2×10^{-4}
^{208}Tl	Surface	1.2×10^{-4}
^{60}Co	Crystal	4.7×10^{-5}

Table 3: Fraction of radioactive decays that deposit an energy within a ± 5 keV window around $Q_{\beta\beta}$ in one segment only in germanium detector array of 21 crystals of 2 kg each, with a $6_\phi \times 3_z$ segmentation scheme.

7.4 Other studies

Simulations of ^{60}Co contaminations internal to the crystals of segmented detectors operated in liquid argon with simultaneous scintillation light readout show that the background suppression methods by segmentation and by scintillation are orthogonal to each other (ie. the suppression factors are multiplicative). For example, a single crystal with seven-fold horizontal segmented operated in liquid argon, exhibits a combined reduction factor of 10^3 at $Q_{\beta\beta}$.

Other ongoing studies include the simulation of calibration sources to determine their source strength and position and the simulation of ambient neutron background.

8 Material screening

The techniques available in Gerda for the search of ultrapure materials required for the detector construction include low-level germanium gamma spectrometry (MPIK, LNGS, Baksan); instrumental neutron activation analysis (INAA) (Pavia/LNGS); inductively coupled plasma mass spectrometry (ICPMS) (LNGS); radon emanation measurements (MPIK, Moscow) as well as alpha and beta spectrometry (Cracow). Recently, a new group (M. Hult) at the Institute for Reference Materials and Measurements (IRMM) in Geel (Belgium) joined the Gerda Collaboration. This group operates three low-level Germanium gamma ray spectrometers in the underground laboratory HADES, located in Mol (Belgium), thus substantially enlarging the capabilites of Gerda for material screening.

8.1 Assay of bulk impurities

In the reporting period, contamination measurements on a variety of sample have been performed. So far, these measurements have been done at MPIK, LNGS and Baksan. At MPIK and LNGS we have measured many materials which are required for the construction of the copper cryostat as well as materials for the detector suspension and the electrical connection and insulation. In copper-stannous welding-rods traces of radium were detected.

Therefore the GERDA cryostat will be electron beam welded. A more serious problem is the electrical connections to the detectors. The measured Kapton cable was found to be high in radium. Here we are planning to measure samples of pure Kapton in order to select the appropriate raw material. A very detailed study of radioactive contaminations in all parts of photomuliplier tubes was performed. The results were used to optimize the design of the LARGE shielding system. At Baksan measurements of radioactive contamination of materials for GERDA have recently been started in the low background underground facility of the Baksan Neutrino Observatory. A sample of a CuP alloy (which is required as an addition to the copper for the cryostat) has been placed into the 4-HPGe spectrometer setup.

In cases where only small samples of the material under consideration are available, ICPMS and INAA are possible alternatives to low-level gamma ray spectroscopy. First INAA measurements on two samples (Teflon, Torlon) have been performed at the LENA reactor in Pavia. Concerning the ICPMS technique, an ICPMS instrument is available at LNGS for use in GERDA. In addition, the MPIK group has initiated a collaboration with the Institute for Mineralogy, University of Frankfurt (Germany), where ICPMS is routinely applied. The suitability of different samples for ICPMS measurements (steel plates, soldering wires, Cu-Be contacts, photomultiplier glass, CuP alloy, Kapton cable, Torlon plates, super insulation foil) which partly have been already measured with gamma ray spectroscopy at MPIK and at LNGS is currently investigated. Since INAA and ICPMS measure the long-lived parent isotopes they give complementary informations to the gamma spectroscopy results which are useful to study the mechanisms which can break the secular equilibrium.

8.2 Assay of surface contaminants

We are also preparing tests to measure the efficiency of different copper surface purification procedures by means of the radon emanation technique. A 250 m^3 copper tape has been purchased for that purpose and purity levels below 1 μBq/m^3 in terms of ^{222}Rn emanation rates will be detectable. It is important to prove that chemicals which are used for etching and electropolishing do not re-contaminate the surfaces. Therefore measurements of polonium deposition on copper surfaces were started at Cracow.